ELSEVIER

Marine Geology 224 (2005) 145–156

MARINE GEOLOGY
INTERNATIONAL JOURNAL OF MARINE GEOLOGY, GEOCHEMISTRY AND GEOPHYSICS

www.elsevier.com/locate/margeo

Transport of gravel and cobble on a mixed-sediment inner bank shoreline of a large inlet, Grays Harbor, Washington

Philip D. Osborne *

Pacific International Engineering, PLLC, 123 Second Ave. South, P.O. Box 1599, Edmonds, WA 98020, USA

Received 29 April 2005; received in revised form 12 August 2005; accepted 19 August 2005

Abstract

Gravel and cobble transport measurements were obtained by particle tracing experiments from a mixed sand, gravel and cobble beach at the head of a crenulate-shaped shoreline, Half Moon Bay in Grays Harbor, Washington. The direct measurements and results provide insight regarding the differential transport of gravel and cobble sized material on mixed-sediment beaches. The results are of relevance to the development of both predictive formulae for coarse-grained sediment transport and guidance for practical gravel and cobble beach design. Net alongshore transport of gravel and cobble is generally several times greater than the net cross-shore transport at Half Moon Bay. Larger and smaller particles both move preferentially alongshore; however, smaller particles tend to move across-shore more than larger particles. Particle transport distance during a tidal cycle increases with particle size (or mass) up to a point, beyond which the particle transport rate begins to decrease with increasing size. The direct relationship between transport rate and particle size may reflect the selective entrainment and the rejection (or overpassing) of larger particles, which are more exposed to fluid forces on the beach surface than smaller particles, which are sheltered within the matrix of larger particles, as well as the higher susceptibility to burial of smaller particles. The decrease in transport rate for the largest sizes may reflect the limited competency of the fluid forces to transport larger and heavier particles under the observed conditions. The direct transport measurements are consistent with the overall particle size and shape distributions observed on this crenulate-shaped inner bank beach whereby the larger and flatter particles have tended to outrun the smaller and more spherical particles in the downdrift direction.

Keywords: mixed grain beach; crenulate bay; gravel/cobble transport; longshore transport; cross-shore transport; beach erosion

1. Introduction

Most nearshore sediment transport research has been focused on open coast beaches composed of sand-sized sediment. Modes, mechanisms and rates of transport of coarse bedload on gravel (includes granules and pebbles of the Wentworth size classes) and cobble beaches and mixed sand and gravel beaches remain relatively poorly understood. Predictions of coarse-grain transport are often unreliable because of a lack of high quality field data from gravel and cobble and mixed grain beaches to test predictions of sediment transport and mobility (Bradbury and McCabe, 2003). Furthermore, no existing transport model contains the most significant factors for coarse-grained and mixed grain sediment transport which should include swash and backwash hydrodynamics, infiltration, steep beach gradients, fraction-

* Tel.: +1 425 921 1720; fax: +1 425 744 1400.
E-mail address: philo@piengr.com.

0025-3227/$ - see front matter
doi:10.1016/j.margeo.2005.08.004

ation and differential hydraulic conductivity (e.g. Quick and Dyksterhuis, 1994; Van Wellen et al., 2000; Mason and Coates, 2001).

Mixed grain beaches are widespread, particularly in mid to northern latitudes including England, Ireland, Canada, New Zealand, and parts of the United States (e.g. Carter et al., 1990; Kirk, 1969). Mixed grain beaches, in particular, are recognized as being morphologically distinct from and more complex than either sand or gravel beaches (Kirk, 1980), but relatively little is known about the basic factors that distinguish processes of sediment transport on mixed beaches from those on single sediment beaches (Mason and Coates, 2001).

Difficulties arise with obtaining field measurements of sediment transport and the forcing hydrodynamics on mixed beaches because of a lack of instruments capable of direct measurements in an energetic swash zone in which large cobbles and gravel particles are in motion. Experiments to measure transport on coarse-grained beaches are generally limited to laboratory studies (e.g. Coates, 1994; Quick and Dyksterhuis, 1994), tracer studies (e.g. Nicholls and Wright, 1991; Van Wellen et al., 2000), or transport has been inferred from morphology changes (e.g. Galster and Schwartz, 1990) or from alongshore and cross-shore sediment size and shape distributions (e.g. Komar, 1977). Despite the lack of data and predictive ability for coarse-grained and mixed beaches, there is significant demand for design guidance on gravel and cobble and mixed beaches owing to their relative efficiency at dissipating wave energy and providing a natural or managed coastal defence (e.g. Bradbury and McCabe, 2003; Komar et al., 2003).

A crenulate beach formed on the sandy inner bank of a large tidal inlet (Seabergh, 2002) that has been nourished with gravel and cobble provides an opportunity to examine rates and patterns of sand, gravel and cobble transport in a relatively sheltered wave environment. Systematic variations in wave height and wave angle occur alongshore on a crenulate beach as a result of wave diffraction, affording a wider range of experimental conditions within a relatively small spatial and temporal extent than could be achieved on an open coast beach.

This paper presents gravel and cobble transport measurements obtained through a series of field experiments on a mixed sand, gravel and cobble transition beach at the head of a crenulate-shaped bay, Half Moon Bay, Grays Harbor, Washington. Measurements were obtained during two particle tracer deployments in 2003 and 2004. The tracer technique involved a combination of magnetic detection of tracer particles and Real Time Kinematic Global Positioning System (RTK-GPS) surveying. The tracer measurements and surveying permit an assessment of cross-shore and alongshore transport rates and provide insight regarding the differential transport of different sized material on this beach. The results provide data that are useful for the long-term management of a nourished section and provide fundamental data for the development and testing of transport predictive formula.

2. Study location and physical setting

Jetties at inlets often terminate in the alluvial soil of the barrier island or mainland of the entrance that they stabilize. The termination area, exposed to waves and currents is frequently observed to erode and a crenulate shaped shoreline will develop from the terminus of the jetty extending both bayward and laterally into the barrier (Seabergh, 2002). The planform shape of such beaches is primarily the result of wave diffraction caused by the structure or headland, in this case the landward terminus of the jetty.

Half Moon Bay at Grays Harbor, Washington (Fig. 1) is an example of a crenulate-shaped shoreline that has formed on the inner bank of a tidal inlet. Erosion of the Half Moon Bay shoreline at the landward end of the south jetty at Grays Harbor resulted in a breach between the jetty and the adjacent south beach shoreline during a 10 December 1993 winter storm. The repair included a sand fill for the breach, a wave diffraction mound at the east end of the jetty, and placement of a mixed, gravel and cobble transition beach on the breach fill in Half Moon Bay adjacent to the wave diffraction mound (Fig. 2). The breach area was filled with dredged sand in 1994 and the diffraction mound and transition beach were placed in 1999. Continuing erosion of the shoreline has prompted further study of the shoreline and a long-term solution to address the erosion is sought. The history of the project and engineering features are described in greater detail in Osborne et al. (2003).

Grays Harbor is located on the southwest Washington coast at the mouth of the Chehalis River, approximately 70 km (45 miles) north of the Columbia River entrance and 180 km (110 miles) south of the Strait of Juan de Fuca. The pear-shaped harbor is 18 km (11 miles) wide and 24 km (15 miles) long. The estuary is enclosed on the ocean side by spits, Point Brown on the north and Point Chehalis on the south. The spits are separated by a 2-mile-wide opening, which forms the natural harbor entrance. Two convergent rock jetties, north jetty and south jetty, extend seaward from the spit

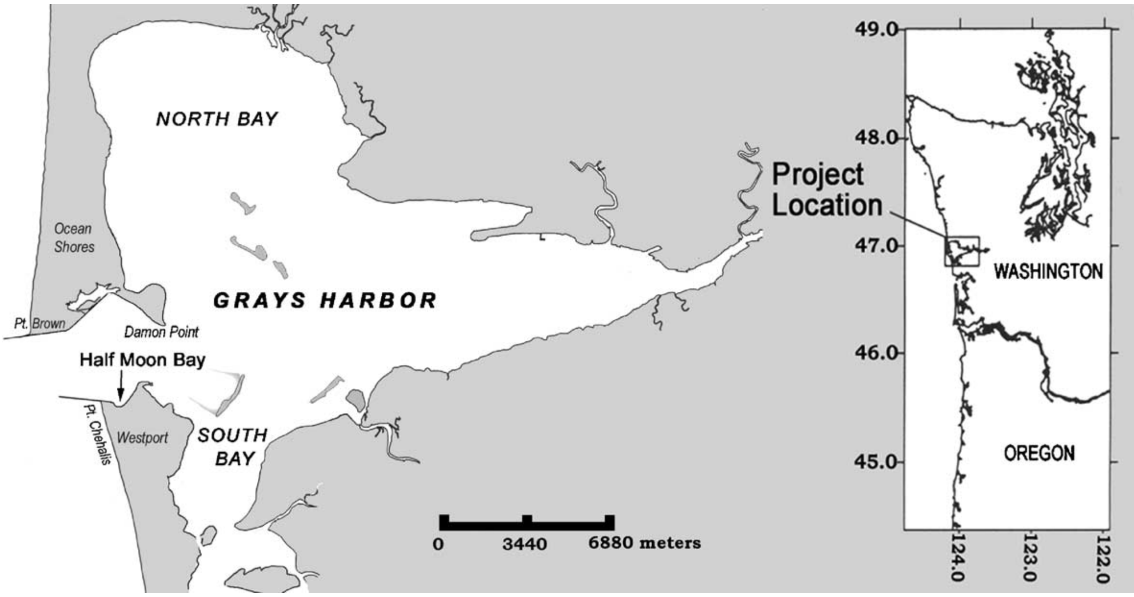

Fig. 1. Location of Half Moon Bay, Grays Harbor, WA.

points. The jetties are part of the Grays Harbor navigation project, which is a Federally constructed and maintained navigation channel that allows deep-draft shipping through the outer bar, Grays Harbor estuary, and the Chehalis River to Cosmopolis. The harbor entrance is exposed to an energetic wave climate dominated by storm waves and swell from the Pacific Ocean (Osborne, 2003).

Fig. 2. Location of engineering measures to prevent breaching at South Jetty Grays Harbor including breach fill, diffraction mound and mixed gravel and cobble transition beach (date of photo: 29 December 2003).

3. Methods

The experimental layout for the field measurements is shown in Fig. 3. Measurements include sampling of sediments for bed material characterization and tracer grain preparation, tracer grain experiments, beach profile surveying, and wave and current measurements.

3.1. Bed material characterization and tracer grain preparation

Size distributions of the transition beach sediments were characterized by sampling the surface and subsurface sediments. Surface samples were acquired to obtain tracer particles and to examine any horizontal variations in size and shape characteristics on the transition beach. Subsurface sampling was conducted to examine any vertical variations in bed material composition. Because of the large number and volume of samples required for characterization of gravels and cobbles, sieve analysis was not practical for all surface samples of the material.

The design specification for the gravel and cobble transition beach is shown in Table 1. Surface and subsurface bed material were characterized by volumetric bulk sampling analysis using field sieving for the coarse cobble fraction and standard laboratory sieving for the finer fraction. Sediment samples were acquired from the transition beach in June 2002 for analysis.

Table 1
Size distribution specification for gravel and cobble on the transition beach

US standard sieve size (mm (in.))	Size (ϕ)	Percent passing by weight
304.8 (12)	−8.3	100
152.4 (6)	−7.3	85–100
76.2 (3)	−6.3	50–85
19.1 (3/4)	−4.3	0–40
9.5 (3/8)	−3.2	0–6
0.074 (0.003)	3.8	0–3

Shore material gradation was determined at a series of transects coinciding with regular beach profile monitoring surveys shown in Fig. 3. The gradation of material at transects 2, 3, and 4 in the transition beach region is listed in Table 2. The proportion of sand varies with distance below the surface and also with position on the profile. At lower elevations on the beach the higher percentage of sand results in a lower beach slope. Higher on the beach profile, there is a higher proportion of gravel and the beach steepens.

Surface gravel and cobble material were sampled using the grid-by-number method (Wolman, 1954). The grid-by-number method is the most widely used sampling technique for coarse bed surfaces (e.g. Rice and Church, 1996) and involves the determination of the relative area covered by grain sizes rather than their relative weight. The method involves establishing a grid on the beach surface and sampling the grains

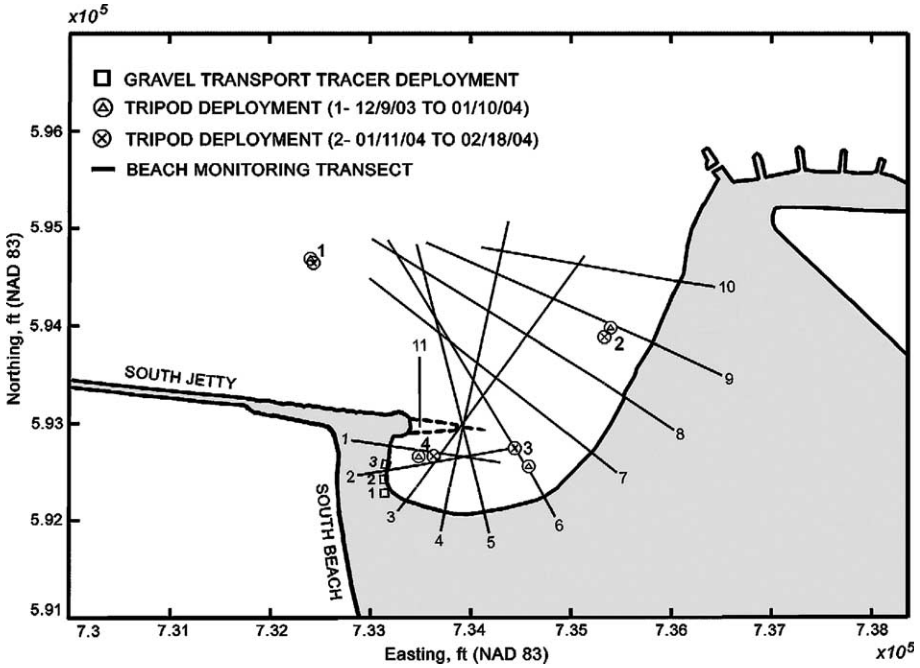

Fig. 3. Experimental layout for field measurements in Half Moon Bay.

Table 2
Gradation of shore material in western end of Half Moon Bay

Transect	Source	Elevation (m (ft))	Gravel cobble (%)	Sand (%)	Fines (%)
2	Surface	0.91 (3)	33.9	65.9	0.2
2	Subsurface	0.91 (3)	21.4	77.8	0.8
3	Surface	0.91 (3)	5.2	93.3	1.5
3	Subsurface	0.91 (3)	0.2	98.8	1
4	Surface	0.91 (3)	13.1	86.6	0.3
4	Subsurface	0.91 (3)	2.4	97.1	0.5

Date of sampling is 26 June 2002.

lying directly beneath each grid point. Distance between successive samples is no less than three times the diameter of the largest particles and individual grains are characterized by the length of the intermediate axis. Precision of percentile estimates using the Wolman procedure is achieved at the expense of a large sample size. Rice and Church (1996) showed that once sample sizes reach 400 particles the appropriate 95% confidence limits of $\pm 0.1\ \phi$ are reached.

The size distribution of the surface samples was determined by measurement of the lengths of the principal orthogonal axes of the particles: L=long, I=intermediate, and S=short. The size distribution of the surface sample was divided into six size fractions based approximately on the Udden–Wentworth size classification scale and the ϕ size of the particles, where $\phi = -\log_2 (I_{\mathrm{mm}})$, and I_{mm} is the length of the intermediate axis in mm. The size distribution of a surface sample (N=414) of gravel and cobble from the transition beach is shown as a histogram and cumulative frequency curve in Fig. 4.

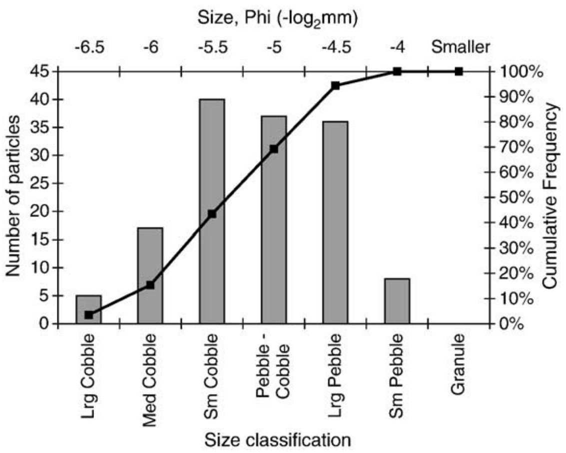

Fig. 4. Size distribution of a surface sample (N=414) of gravel and cobble from the transition beach (August 2003). Size is based on the length of the intermediate axis.

Five particles from each of six size classes were sampled at random from the overall surface sediment sample for each of the tracer particle sets. Small but powerful magnets were attached to each tracer particle with an epoxy and a label for grain identification. The mass and volume of the magnets was small in relation to the mass and size of the tracer particles and therefore the change in specific gravity of the tracer particles is expected to be small or negligible. Each particle was coated with epoxy paint that was color coded by size fraction for easier identification of tracer particles on the beach. The size characteristics of the magnetic tracer particles are summarized in Table 3.

3.2. Gravel and cobble transport measurements

Direct measurements of the transport of pebble and cobble beach sediments have been obtained through particle tracing experiments using painted, magnetized, or tagged particles. Sediment tracing experiments using painted particles often have relatively poor recovery rates (much less than 50%) than limit the value of quantitative information that can be derived from the effort. Recently the development of methods based on magnetized particles has allowed the motion of pebble and cobble particles to be studied with more precision (e.g. Hassan and Church, 1992; Nicholls and Webber, 1987; Voulgaris et al., 1999). A metal detector can be used to locate individual grains resulting in a higher

Table 3
Summary of size classes and average characteristics of magnetic tracer particles

	Size class	L (mm)	I (mm)	S (mm)	m (kg)	ϕ	ψ	Description
Set 1	1	126	107	69	1.471	−6.7	0.71	Large cobble
	2	91	68	44	0.414	−6.1	0.67	Medium cobble
	3	70	52	38	0.201	−5.7	0.73	Small cobble
	4	49	37	20	0.055	−5.2	0.62	Pebble–cobble
	5	38	29	17	0.030	−4.8	0.65	Large pebble
	6	32	20	14	0.012	−4.3	0.67	Small pebble
Set 2	1	134	108	67	1.392	−6.7	0.68	Large cobble
	2	93	69	38	0.376	−6.1	0.61	Medium cobble
	3	66	50	31	0.152	−5.7	0.66	Small cobble
	4	52	38	22	0.061	−5.3	0.63	Pebble–cobble
	5	42	30	20	0.039	−4.9	0.69	Large pebble
	6	33	21	13	0.013	−4.4	0.62	Small pebble
Set 3	1	138	108	74	1.732	−6.8	0.71	Large cobble
	2	103	79	41	0.453	−6.3	0.59	Medium cobble
	3	81	54	36	0.228	−5.8	0.66	Small cobble
	4	50	39	22	0.069	−5.3	0.63	Pebble–cobble
	5	39	29	21	0.034	−4.8	0.72	Large pebble
	6	26	19	12	0.008	−4.3	0.65	Small pebble

Table 4
Average wave parameters during particle tracer analysis: 17–19 December 2004

Station	Average H_s (m)	Average T_p (sec)	Average D_p (deg-T)
CDIP	3.38	15.5	268.9
HM1	1.23	14.6	279.7
HM2	1.14	14.3	294.6
HM3	0.73	17.2	320.3
HM4	0.45	16.6	359.7

recovery rate. In this study, the tracer technique involved a combination of magnetic tracer particles and surveying with Real Time Kinematic Global Positioning System (RTK-GPS). The RTK-GPS enabled location of the tracer particles with horizontal accuracy of approximately ± 10 cm and vertical accuracy of ± 5 cm. A field calibration of the RTK GPS was conducted to reduce discrepancies between local control and GPS-derived coordinates. This was accomplished by centering the GPS antenna over at least 4 known monuments in the area and recording data for a period of time. The surveyed positions are then spatially adjusted to convert the GPS-derived coordinates to local coordinates.

The tracer experiments described in this paper involved three sets of magnetic particle tracer deployments on 17 December 2003 and 9 February 2004. The first set (Set 1) was deployed on 17 December 2003 and re-surveyed during the two successive high tides between 17 December and 19 December 2003. Sets 2 and 3 were deployed on 9 February 2004 and measured during the successive high tides between 9 February and 13 February 2004.

3.3. Tracer grain placement

A series of six, approximately shore normal transects were established at approximately 2-m alongshore intervals within the upper inter-tidal zone of the transition beach for the placement of tracer particles. Five particles from each size class were placed along each of the six shore-normal transects at elevations between +0.6 m, mllw and +1.8 m, mllw at intervals of approximately 0.3 m vertical. At each position, a particle of approximately equal size was removed from the bed and replaced with the tracer particle, with care to minimize bed disturbance. Initial location of each particle was surveyed using RTK-GPS.

Fig. 3 shows the placement location of tracer particles during the tracer deployments on 17 December 2003 and 9 February 2004. The rectangles in Fig. 3 represent the matrix outlines used to situate the particles at their initial positions. Each particle was placed an equal distance apart in a 6.1 m by 7.3 m approximately sized matrix. During the first deployment, a single set (Set 1) of thirty tracer particles (five particles in six size classes) was deployed. During the second deployment two sets (Sets 2 and 3) of thirty tracer particles were deployed.

3.4. Tracer recovery

The tracer particles were relocated visually and with a magnetic detector after each diurnal tidal cycle. Each particle was positively identified by its painted color and unique numeric label. The particle depth below surface was recorded with a graduated scale. Particle positions were determined by surveying with RTK-GPS.

Upon re-location and identification the particle was lifted to the beach surface at the new location and left on the surface for the next tidal cycle. Beach profiles were surveyed using RTK-GPS to record significant changes in beach profile shape and volume displacements of sediment. Two tracer particles were not recovered during the experiment; recovery was 93%.

3.5. Wave and current measurements

A measurement program was designed to obtain detailed measurements of directional waves, currents, and suspended sediment in Half Moon Bay concurrent with particle tracer measurements. Oceanographic instruments were deployed between 9 December 2003 and 19 February 2004.

Measurements include directional waves, currents, and suspended sediment concentrations in the nearshore zone of Half Moon Bay and in the entrance to Grays Harbor. The field data collection effort involved the deployment of four instrument platforms (HM1–4) at locations shown as tripod deployments in Fig. 3. The data collection was scheduled to occur during two months of the winter storm season, with the platforms

Table 5
Average wave parameters during particle tracer analysis: 9–13 February 2004

Station	Average H_s (m)	Average T_p (sec)	Average D_p (deg-T)
CDIP	2.01	12.8	271.1
HM2	0.87	13.0	291.0
HM3	0.57	13.1	312.2
HM4	0.38	12.9	343.3

Table 6
Statistical summary of cobble measurements at Half Moon Bay

Transect		L (mm)	I (mm)	S (mm)	ψ	L/S
1	Mean	40.35	28.81	17.51	0.64	2.37
	Median	40	28	17	0.64	2.32
	S.D.	8.35	6.77	3.31	0.11	0.60
	Count	37	37	37	37	37
	95% CI	2.69	2.18	1.07	0.04	0.19
3	Mean	62.92	46.68	26.47	0.62	2.61
	Median	61	44	26	0.62	2.50
	S.D.	12.99	12.42	9.10	0.14	0.91
	Count	53	53	53	53	53
	95% CI	3.50	3.34	2.45	0.04	0.24
5	Mean	92.09	70.71	35.13	0.57	2.77
	Median	89	67	33	0.57	2.70
	S.D.	25.07	21.63	11.70	0.12	0.83
	Count	56	56	56	56	56
	95% CI	6.57	5.66	3.06	0.03	0.22

being deployed for two consecutive 30-day periods. The tripod at HM1 was equipped with an RD Instruments Sentinel Workhorse ADCP to measure directional wave spectra inside the inlet entrance and approaching Half Moon Bay. Platforms at HM1–3 were equipped with Sontek Hydra systems including Acoustic Doppler Velocimeters, Paros Pressure sensors, and Optical Backscatterance Sensors. A directional wave buoy maintained by the US Army Corps of Engineers also measured waves outside the entrance to Grays Harbor.

Time-averaged descriptive wave parameters including significant wave height, H_s, peak period, T_p, and peak wave direction, D_p, measured at Half Moon Bay during the two tracer deployments are summarized in Tables 4 and 5. Offshore waves were measured at a wave buoy operated by the Coastal Data Information Program (CDIP 036) located at 43 m depth approximately 1 km southwest of the entrance to Grays Harbor. Waves during the deployments are characteristic of average winter conditions with an average H_s of 3.4 m and T_p of 15.5 sec from the west and west–southwest. However, the wave heights and periods were greater during the first deployment, which contributed to the increased particle displacement. Systematic spatial variations in wave height and direction reflect the shoaling transformations, refraction and diffraction that occur as ocean waves enter Half Moon Bay. Waves are turned from westerly to northwesterly as they enter the inlet (CDIP to HM1) and to northerly (HM1 to HM4) by refraction as they pass the terminus of south jetty. Waves are smallest at HM4 in the immediate lee of the jetty terminus and increase with distance along the crenulate bay shoreline progressing from HM4 to HM2.

4. Cobble size and shape at Half Moon Bay

A number of studies (e.g. Bluck, 1967; Orford, 1975; Sherman et al., 1993) have documented the tendency of gravel and cobble beaches to move towards discrete facies organisation when the effective particle size and sphericity are of sufficient range to allow combination into discrete behavioural units. To provide a preliminary indication of the degree of facies organization present at Half Moon Bay, samples of the cobble on the gravel and cobble transition beach were obtained using the Wolman method on 29 May 2003 at the high water mark at transects 1, 3, and 5. The sampling permitted an analysis of the horizontal variation in cobble size and shape in the transition area and along Half Moon Bay beach. Maximum-projection sphericity,

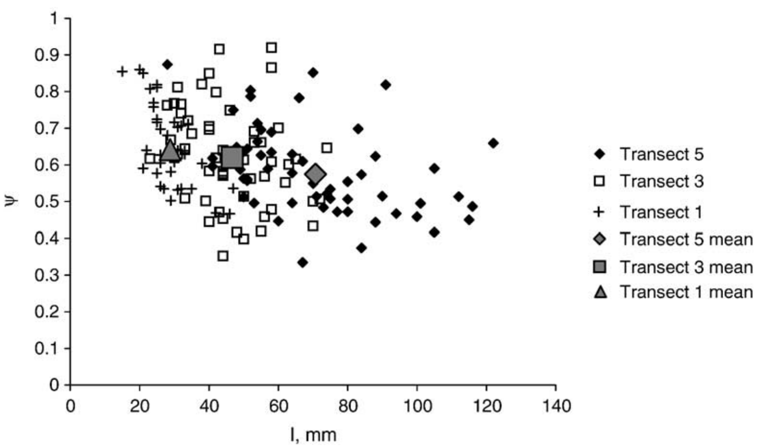

Fig. 5. Particle sphericity as a function of intermediate axial length.

ψ, of the particles determined according to Sneed and Folk (1958) is calculated as:

$$\psi = \left(S^2/IL\right)^{0.33}$$

ψ indicates how closely a particle approximates a sphere by the ratio of the maximum-projection area of the particle to that of a perfect sphere.

Table 6 is a statistical summary of the cobble dimensions and ψ at each transect. Fig. 5 shows the relationship between particle size, represented by the intermediate axial length, and ψ at each of the three cross-sections. The summary and Fig. 5 indicate that there is a significant increase in the average size of the cobbles from transects 1 to 5, as indicated by the 95% confidence intervals about the mean. In contrast, there is a progressive decrease in ψ from transects 1 to 5 indicating that the particles are less spherical as well as larger with distance eastward from the jetty terminus. This corresponds with the visual observation that particles become flatter and more disc-shaped between transects 1 and 5. Note that the standard deviation, an indicator of the relative sorting, increases from transects 1 to 5 indicating that particles are better sorted at transect 1 than at 5.

5. Particle tracer results

Fig. 6 shows the particle transport paths for Set 1 that occurred during the two successive high tides between 17 December and 19 December 2003. The transport paths indicate a net transport alongshore to the south and east. The net alongshore transport is generally several times greater than the net cross-shore transport. Figs. 7 and 8 show the particle paths for transport that occurred for Sets 2 and 3 during the second tracer deployment between 9 February and 13 February 2004.

Fig. 9 shows the mean particle transport distance per diurnal tidal cycle as a function of the particle mass. The particle transport distance is an inverse function of particle size (or mass), with larger particles being transported greater distances in each tidal cycle. This somewhat counter-intuitive relationship may reflect the selective entrainment and over-passing of larger particles, which are more exposed to fluid forces on the

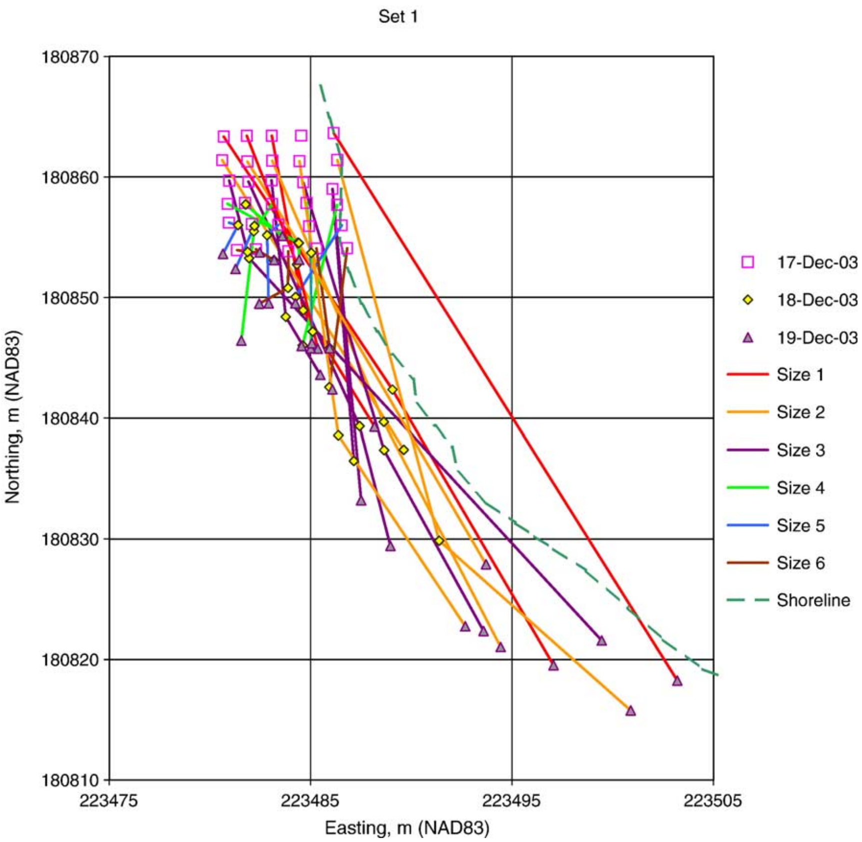

Fig. 6. Particle transport paths for difference size classes in Set 1 between 17 December 2003 and 19 December 2003.

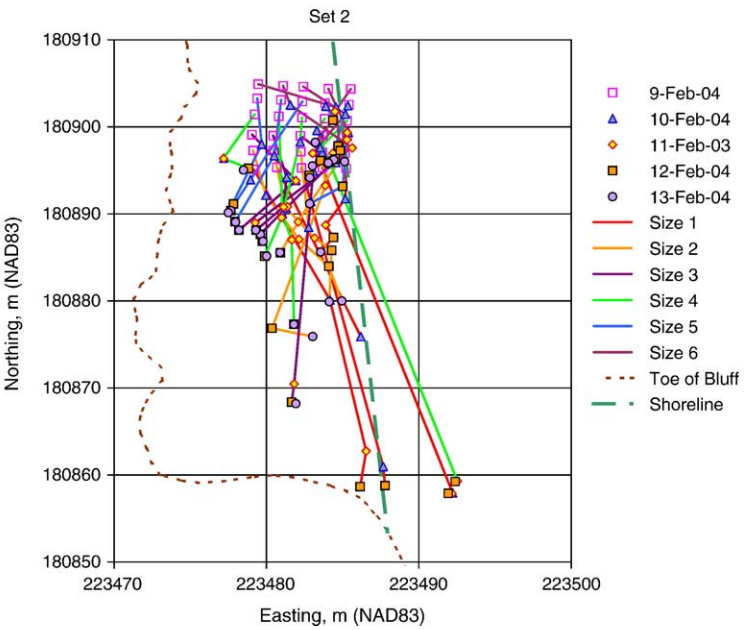

Fig. 7. Particle transport paths for different size classes in Set 2 between 9 February 2004 and 13 February 2004.

surface than smaller particles, which are sheltered within the matrix of larger particles. At a point between the 0.2 kg (54 mm) and 0.4 kg (70 mm) size particles, the particle transport rate begins to decrease with increasing size, most likely reflecting the limited competency of the fluid forces to transport larger and heavier particles under the observed conditions.

Fig. 10 shows the mean depth of burial of particles as a function of particle mass. The results are consistent between sets and illustrate that the smaller particles are more susceptible to burial than the larger particles. The smaller particles in Set 1 were buried to greater depth than similar sized particles in Sets 2 and 3. The greater depth of burial is most likely owing to the more ener-

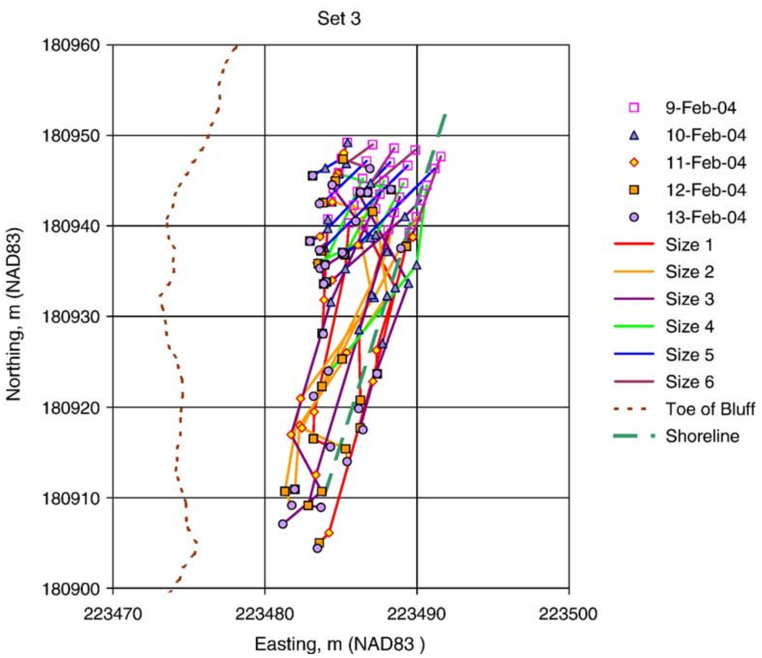

Fig. 8. Particle transport paths for different size classes in Set 3 between 9 February 2004 and 13 February 2004.

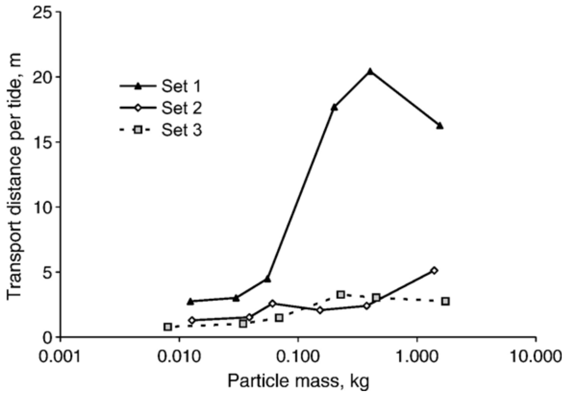

Fig. 9. Transport distance per diurnal tidal cycle as a function of particle mass.

getic waves during the Set 1 measurements causing a greater active transport depth than for Sets 2 and 3. The larger waves also correlate with significantly larger transport rates for the larger particles in Set 1 relative to Sets 2 and 3 in Fig. 9. One data point in Set 2 is an outlier from the remainder of the data set and that is the large burial depth associated with the largest particle size. The largest particles in Set 2 were transported beyond the end of gravel and cobble beach into an area of new sandy beach fill and these particles became deeply buried in the sand fill. Once buried in the sand fill, the particles were no longer actively transported.

The exposed cobble and gravel particles on the surface of the transition beach are relatively mobile alongshore under average winter waves. The particle transport results suggest a significant mass flux of cobble is occurring out of the transition beach area in the southwest corner of the bay to the east along the Half Moon Bay shoreline. This mass flux is confirmed by visual observations and surveys of beach profiles in the transition beach area.

Profile change in the transition beach indicates a net loss of cobble-gravel from the transition beach of 9.4

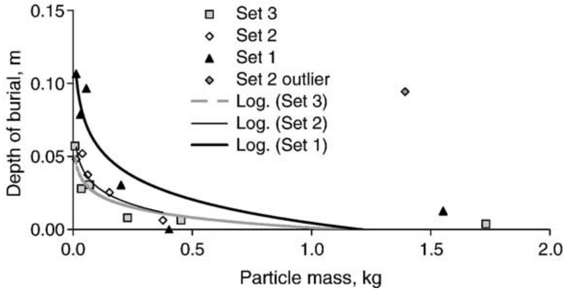

Fig. 10. Depth of burial as a function of particle size expressed in terms of the intermediate axis length (17 December 2003 to 19 December 2003).

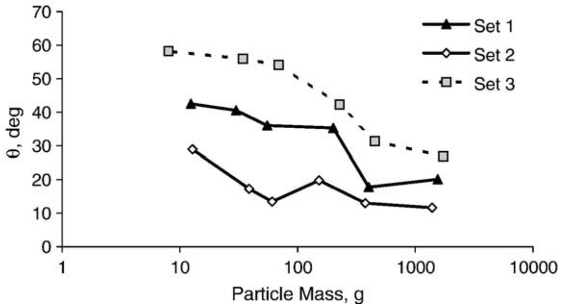

Fig. 11. Average angle between particle trajectory and relative shoreline in relation to particle mass (9 February 2004 through 13 February 2004).

m^3/m of beach above mllw between mid-October and mid-December 2003. Visual observations during the same interval indicated that cobble migrated east from the transition beach area and was deposited at the base of a temporary erosion protection scheme installed by the City of Westport.

The angle between the transport direction and the local shoreline orientation was calculated using Cartesian vector geometry to analyze the relationship between particle mass and transport direction. The angle was calculated for each particle, then an average angle was calculated for each particle size over the respective periods of measurement. Following this scheme, a particle moving parallel to the local shoreline will result in angles approaching zero, while particles moving perpendicular to the shore will result in angles approaching 90°. Fig. 11 shows the relationship between particle trajectory angle and particle mass. All of the particle movement occurred at angles less than approximately 60° with most trajectories less than 45° but greater than 10° indicating a predominance of alongshore transport. An apparent trend is evident in which the particles of larger mass tend to move long-shore (smaller angles) more than the smaller particles, while the particles with smaller mass have more tendency to move in the cross-shore direction (larger angles).

6. Summary and interpretation

Gravel and cobble transport measurements were obtained from the surface of a mixed sand, gravel and cobble transition beach at the head of a crenulate shaped bay, Half Moon Bay, located on the inner bank of the entrance to Grays Harbor, Washington. The transport measurements were achieved by magnetic detection of tracer particles and surveying particle position with a Real Time Kinematic Global Positioning System (RTK-GPS) through time. The measurements permit an assessment of cross-shore and alongshore transport rates of surface particles and provide insight regarding the differential transport of different sized material on this beach. Gravel and cobble samples were also obtained to examine alongshore variations in gravel and cobble size and shape in relation to transport patterns. An array of wave and current sensors provided information of forcing conditions during the experiments.

The measurements of gravel and cobble particle movement indicate that net alongshore transport of gravel and cobble is generally several times greater than the net cross-shore transport at Half Moon Bay. Smaller particles tend to move across-shore more than larger particles which are preferentially moved alongshore. Particle transport distance during a tidal cycle increases with particle size (or mass) up to a point. Beyond a certain size, the particle transport rate begins to decrease with increasing size most likely reflecting the limited competency of the fluid forces to transport larger and heavier particles under the observed conditions. The direct relationship between transport rate and particle size may reflect selective entrainment and rejection (or overpassing) of larger particles, which are more exposed to fluid forces on the surface than smaller particles, which are sheltered within the matrix of larger particles. Smaller particles also exhibit more susceptibility to burial than the larger particles.

The results of a particle shape analysis along the high water shoreline at Half Moon Bay are consistent with the observation that larger particles and disc-shaped particles may outrun smaller, more spherical particles on coarse-grained beaches (e.g. Komar, 1977). It has been argued that this may reflect a propensity for the larger flatter particles to accumulate in the surf and swash zones, while smaller, more spherical particles move seaward more easily by rolling downslope (Lorang and Komar, 1990). Once started, the latter pattern may be reinforced by grain sorting processes that include rejection (overpassing) and impedance: a coarser particle is more likely to be moved out (rejected) of an area that is dominated by smaller well-sorted particles (e.g. Carr et al., 1970; Carr, 1969; Bluck, 1967). Larger flatter particles will tend to roll or slide easily along a well-sorted, more densely packed beach made up of smaller particles. In contrast, transport of smaller particles in an area of mixed sizes tends to be impeded by the larger particles (e.g. Carter, 1988). An overall decrease in sorting and increase in size in the downdrift direction along Half Moon Bay shoreline are consistent with these mechanisms.

The directional transport distribution may also differ for the various size and shape components that comprise the beach sediment. Carter (1988) suggests that under moderate and low energy swell, the smaller-spherical particles set in motion on a steep beach are more likely to be rolled downslope and out of the swash zone, leaving larger discs higher on the beach. Whereas, under more energetic storm waves, the discs and larger particles get selectively transported, preferentially shoreward (e.g. Everts et al., 2002), and also alongshore when there is an angle to wave approach. Sorting and shoreward transport of cobbles can also be explained through an understanding of wave orbital velocity asymmetry under shoaling waves. The highest water particle velocity is under the crest of a shoaling wave when the water is moving shoreward. Under the trough of a shoaling wave the water velocity is directed seaward and is smaller in magnitude. The higher velocity shoreward flow is able to move cobbles. However, the lower velocity seaward flow is preferentially not able to move cobbles. As a consequence, the cobbles tend to move onshore.

It could be argued that particle shape (e.g. sphericity) may also be a decisive factor, in addition to grain size, in determining the larger scale and longer term transport patterns of coarse-grained sediments at Half Moon Bay. In this study, tracer particles were selected at random from a sample of beach sediments which was deemed to be representative of the range in variations in both particle size and shape variations present on the section of the beach where the tracers were eventually deployed. The analysis of size and shape variation on the beach demonstrates that there is a statistically significant variation in particle size within the section of beach where the transport measurements were obtained but not a significant variation in sphericity. Therefore, it seems more likely that the dominant trends in transport rate at Half Moon Bay are most strongly associated with particle size rather than particle shape. Further, it has been suggested by Carter and Orford (1993) that facies development on coarse-grained beaches may be an indication of the transition from longshore dominated (drift alignment) to cross-shore dominated (swash aligned) systems. However, it is important to recognize that the cobble and gravel present on Half Moon Bay originated as an unsorted, artificial placement of non-native sand, gravel, and cobble in the southwest corner of a crenulate-shaped bay that had originally developed on a predominately sandy substrate. It is apparent from the transport observations described in this paper that the gravel placement is predominately being modified by alongshore transport despite the fact that the overall shape of beach may be tending strongly towards swash-alignment.

The three sets of field measurements obtained in this study exhibit consistent trends which support many of the above observations and ideas concerning sorting of gravel and cobble under waves. The challenge remains to incorporate these processes into quantitative predictive models for sediment transport on mixed grain beaches.

Acknowledgements

Funding for the field experiments was provided by ERDC-CHL (The US Army Corps of Engineers Engineer Research and Development Center-Coastal Hydraulics Laboratory) under contract DACW 42-03-C-0028 and a grant from the Coastal Inlets Research Program. The author is grateful to David Hericks, Robert Osborne, and Wei Chen of Pacific International Engineering, PLLC, for assistance with the field measurements and to Dr Nicholas Kraus of ERDC-CHL for useful discussion of the paper. Two anonymous reviewers are to be thanked for providing helpful comments that lead to improvements in the paper.

References

Bluck, B.J., 1967. Sedimentation of beach gravels: examples from South Wales. Journal of Sedimentary Petrology 37, 128–156.

Bradbury, A.P., McCabe, M., 2003. Morphodynamic Response of Shingle and Mixed Sand/Shingle Beaches in Large Scale Tests—Preliminary Observations, Conference Paper—Hydrolab II, Budapest, 22–23 May 2003, pp. 9–1–9–11.

Carr, A.P., 1969. Size grading along a pebble beach; Chesil Beach, England. Journal of Sedimentary Research 39, 297–311.

Carr, A.P., Gleason, R., King, A., 1970. Significance of pebble size and shape in sorting by waves. Sedimentary Geology 4, 89–101.

Carter, R.W.G., 1988. Coastal Environments. Academic Press, London. 617 pp.

Carter, R.W.G., Orford, J.D., 1993. The morphodynamics of coarse clastic beaches and barriers: a long term perspective. Journal of Coastal Research 15, 158–179 (special issue).

Carter, R.W.G., Jennings, S.C., Orford, J.D., 1990. Headland erosion by waves. Journal of Coastal Research (6), 517–529.

Coates, T.T., 1994. Effectiveness of control structures on shingle beaches: physical model studies, HR Wallingford Report SR 387.

Everts, C.H., Eldon, C.D., Moore, J., 2002. Performance of cobble berms in Southern California. Shore and Beach 4 (70), 5–14.

Galster, R., Schwartz, M., 1990. Ediz Hook—a case history of coastal erosion and rehabilitation. Journal of Coastal Research 6, 103–113 (SI).

Hassan, M.A., Church, M., 1992. The movement of individual grains on the stream bed. In: Billi, P., Hey, R.D., Thorne, C.R., Tacconi, P. (Eds.), Gravel-bed Rivers. John Wiley & Sons, pp. 159–175.

Kirk, R.M., 1969. Beach erosion and coastal development in the Canterbury Bight. New Zealand Geographer 25, 23–35.

Kirk, R.M., 1980. Mixed sand and gravel beaches: morphology, processes and sediments. Progress in Physical Geography 4, 189–210.

Komar, P.D., 1977. Selective longshore transport rates of different grain-size fractions within a beach. Journal of Sedimentary Research 47, 1444–1453.

Komar, P.D., Allan, J.C., Winz, R., 2003. Cobble beaches—the design with nature approach for shore protection. Proceedings of Coastal Sediments '03, Clearwater Beach, FL. Available on CDROM.

Lorang, M.S., Komar, P.D., 1990. Pebble shape. Nature 347, 433–434.

Mason, T., Coates, T.T., 2001. Sediment transport processes on mixed beaches: a review for shoreline management. Journal of Coastal Research 17 (3), 645–657.

Nicholls, R.J., Webber, N.B., 1987. Aluminum pebble tracer experiments on Hurst Castle Spit. Proc. Coastal Sediments '87. ASCE, pp. 1563–1577.

Nicholls, R.J., Wright, P., 1991. Longshore transport of pebbles: experimental estimates of *K*. Proc. Coastal Sediments '91. ASCE, pp. 920–933.

Orford, J.D., 1975. Discrimination of particle zonation on a pebble beach. Sedimentology 22, 441–463.

Osborne, P.D., 2003. Dynamics of a remnant flood shoal in a large jettied inlet, Grays Harbor, Washington. Proceedings of the Canadian Coastal Conference, Kingston. Available on CD-ROM.

Osborne, P.D., Wamsley, T.V., Arden, H.T., 2003. South jetty sediment processes study, Grays Harbor Washington: evaluation of engineering structures and maintenance measures, US Army Corps of Engineers, Engineering Research and Development Center, Coastal and Hydraulics Laboratory, ERDC/CHL TR-03-4.

Quick, M.C., Dyksterhuis, P., 1994. Cross-shore transport for beaches of mixed sand and gravel. International Symposium: Waves—Physical and Numerical Modeling. Canadian Society of Civil Engineers, pp. 1443–1452.

Rice, S., Church, M., 1996. Sampling surficial fluvial gravels: the precision of size distribution percentile estimates. Journal of Sedimentary Research 66 (3), 654–665.

Seabergh, W.C., 2002. Inner bank erosion processes and solutions at coastal inlets. US Army Corps of Engineers, ERDC/CHL–CHETN-IV-52.

Sherman, D.J., Orford, J.D., Carter, R.W.G., 1993. Gravel beach-cusp sedimentation: size and shape sorting. Sedimentology 40, 1139–1152.

Sneed, E.D., Folk, R.L., 1958. Pebbles in the Lower Colorado River, Texas: a study in particle morphogenesis. Journal of Geology 66, 114–150.

Van Wellen, E.V., Chadwich, A.J., Mason, T., 2000. A review and assessment of longshore sediment transport equations for coarse-grained beaches. Coastal Engineering (40), 243–275.

Voulgaris, G., Workman, M., Collins, M.B., 1999. Measurement techniques of shingle transport in the nearshore zone. Journal of Coastal Research 15 (4), 1030–1039.

Wolman, M.G., 1954. A method of sampling coarse river-bed material. Transactions-American Geophysical Union 35 (6), 951–956.